1138 (1) Å. $C_{11}H_{18}OS$ has a molecular weight of 198.32 amu, and with $Z = 4$. The calculate density is 1.16 g/cm^3. Data were collected on a Syntex $P2_1$ four-circle diffractometer in the θ-2θ mode using copper radiation, λ 1.5418 Å; 1034 reflections were retained as observed, 250 rejected as unobserved. The structure was solved by direct methods[47] and refined by least-squares methods.[48] The final agreement factors were $R_1 = 0.04$, $R_2 = 0.05$. The final difference map was judged to be free of significant features. Final atomic positional parameters are given in Table V, and the bond lengths and angles are given in Table IV.

Acknowledgment. We are pleased to acknowledge support of this investigation by NSF (Grant CHE-8219093) and NIH (Grant GM 31776-01A1). We thank Regina Zibuck and Professor Amos B. Smith, III, of the University of Pennsylvania for providing several 300-MHz NMR spectra. We thank Dr. Catherine E. Costello, Associate Director of the Massachusetts Institute of Technology Mass Spectrometry Laboratory (NIH Division of Research Resources, Grant No. RR00317 to K. Biemann), for the high-resolution mass spectra.

Registry No. 1, 17649-89-7; **2**, 17649-90-0; **3**, 96898-99-6; **4**, 79300-00-8; **5**, 17649-86-4; **6**, 87615-87-0; **7**, 51507-08-5; **8**, 5780-61-0; **9**, 21441-31-6; **10**, 89489-55-4; **11**, 96899-00-2; **12a**, 96899-01-3; **12b**, 96899-02-4; **13a**, 96899-03-5; **13b**, 96899-04-6; (*E*)-**14**, 96899-05-7; (*Z*)-**14**, 86310-05-6; (*E*)-**15a**, 84308-03-2; (*Z*)-**15a**, 96899-06-8; (*E*)-**15b**, 84308-04-3; (*Z*)-**15b**, 96899-07-9; (*E*)-**15c**, 87615-88-1; (*Z*)-**15c**, 96899-08-0; (*E*)-**15d**, 84308-05-4; (*Z*)-**15d**, 84308-06-5; (*E*)-**15e**, 96899-09-1; (*Z*)-**15e**, 96899-10-4; **16**, 96899-11-5; (*E*)-**17a**, 84308-07-6; (*Z*)-**17a**, 84308-08-7; (*E*)-**17b**, 96899-12-6; (*Z*)-**17b**, 96899-13-7; (*E*)-**17c**, 96899-14-8; (*Z*)-**17c**, 96899-15-9; (*E*)-**17d**, 96899-16-0; (*Z*)-**17d**, 96899-17-1; (*E*)-**18a**, 96899-18-2; (*Z*)-**18a**, 96899-19-3; (*E*)-**18b**, 96899-20-6; (*Z*)-**18b**, 96899-21-7; (*E*)-**19**, 84308-09-8; (*Z*)-**19**, 84308-10-1; (*E*)-**20a**, 86310-01-2; (*Z*)-**20a**, 62453-10-5; (*E*)-**20b**, 86310-02-3; (*Z*)-**20b**, 96899-22-8; (*E*)-**20c**, 96899-23-9; (*Z*)-**20c**, 96899-24-0; (*E*)-**20d**, 96899-25-1; (*Z*)-**20d**, 96899-26-2; **21**, 33944-94-4; (*E*)-**22a**, 86310-03-4; (*Z*)-**22a**, 96899-27-3; (*E*)-**22b**, 86310-04-5; (*Z*)-**22b**, 96899-28-4; (*E*)-**22c**, 96899-29-5; (*Z*)-**22c**, 96899-30-8; (*E*)-**22d**, 96899-31-9; (*Z*)-**22d**, 96899-32-0; **23**, 96899-33-1; (*E*)-**24a**, 87615-89-2; (*Z*)-**24a**, 84308-11-2; (*E*)-**24b**, 96899-34-2; (*Z*)-**24b**, 96899-35-3; (*E*)-**25**, 49784-51-2; (*Z*)-**25**, 49784-64-7; (*E*)-**26**, 96899-36-4; (*E*)-**27a**, 40595-76-4; (*E*)-**27b**, 96899-37-5; (*E*)-**27c**, 96899-38-6; (*Z*)-**27c**, 96899-39-7; **28**, 15904-85-5; (*E*)-**29a**, 96899-40-0; (*Z*)-**29a**, 96899-41-1; (*E*)-**29b**, 96899-42-2; (*Z*)-**29b**, 96899-43-3; **30**, 66716-63-0; **31**, 96899-44-4; (*E*)-**32**, 96899-45-5; (*Z*)-**32**, 96899-46-6; **33**, 96899-47-7; **34**, 96899-48-8; **35a**, 96899-49-9; **35b**, 96899-50-2; i, 96913-37-0; $(CH_3)_2CuLi$, 15681-48-8; $(PhSCuCH_3)Li$, 56831-21-1; $(MeOCMe_2C{\equiv}CCuCH_3)Li$, 79135-33-4; (PhSCuBu)Li, 53128-68-0; $(MeOCMe_2C{\equiv}CCuBu)Li$, 66777-74-0; (PhSCuBu-*sec*)Li, 53972-31-9; (PhSCuBu-*t*)Li, 50281-66-8; $(PhSCuC_3H_5)Li$, 84180-46-1; $(MeOCMe_2C{\equiv}CCuC_3H_5)Li$, 96898-97-4; $(PhSCuCH_2CH_2CH{=}CMe_2)Li$, 61136-35-4; BuCu, 34948-25-9; *t*-BuCu, 56583-96-1; $Ph_3P{\cdot}(CH_3)_2CuLi$, 96898-98-5; $n\text{-}Bu_3P{\cdot}(CH_3)_2CuLi$, 61817-79-6; $[(C_6H_{11})_2PCuCH_3]Li$, 88766-01-2; $[(CH_3)_2CuSCN]Li_2$, 91606-28-9; $[(CH_3)_2CuCN]Li_2$, 80473-70-7; $(CH_3CuCN)Li$, 41753-78-0; EtSH, 75-08-1; $CH_3SSO_2CH_3$, 2949-92-0; 2-formylcyclopentanone, 1192-54-7; (*E*)-2-(methylthiomethylene)cyclopentanone, 82753-83-1.

Supplementary Material Available: Atomic thermal parameters and structure factor tables for (*E*)-**15d** (11 pages). Ordering information is given on any current masthead page.

(47) Main, P. "Multan 78", Department of Physics, University of York, York, England.

(48) Stewart, J. M. "The XRAY System", Technical Report TR-446 of the Computer Science Center, University of Maryland, College Park, MD, version of 1976.

Carbon–Oxygen Bond Cleavage Reactions by Electron Transfer. 2. Electrochemical Formation and Dimerization Reaction Pathways of Cyanodiphenyl Ether Radical Anions

Miles D. Koppang, Neil F. Woolsey, and Duane E. Bartak*

Contribution from the Department of Chemistry, University of North Dakota, Grand Forks, North Dakota 58202. *Received December 7, 1984*

Abstract: The radical anions of 4-cyanodiphenyl ether (**1**) and 2-cyanodiphenyl ether (**2**) have been electrochemically generated and subsequently shown to dimerize in dry *N*,*N*-dimethylformamide (DMF). The radical anion of **1** undergoes irreversible dimerization ($k_2 = 1.1 \times 10^2$ M^{-1} s^{-1}) to form dimeric dianions, which result from coupling either at the 2 and 4 positions or at the 4 and 4 positions with respect to the cyano substituent. The 4–4 coupled dianion undergoes carbon–oxygen bond cleavage with loss of phenoxide ions ($k_1 = 3.8 \times 10^{-2}$ s^{-1}) to form 4,4′-dicyanobiphenyl (**3**). The 2–4 coupled dianion undergoes relatively rapid loss of one phenoxide ion to form an anion, which can be either further reduced to a radical dianion or oxidized in a two-electron process to 2,4′-dicyano-5-phenoxybiphenyl (**4**). The radical anion of **2** reversibly dimerizes ($k_f = 1.2 \times 10^3$ M^{-1} s^{-1}, $k_b = 9.5 \times 10^{-2}$ s^{-1}) to three possible coupled dimeric dianions. Although the 4–4 and 4–6 coupled products (respective to the cyano substituent) are apparently resistant to further reactions, the 2–4 coupled product undergoes loss of phenoxide ion to produce an anion which can be oxidized to 2′,4-dicyano-3-phenoxybiphenyl (**5**).

Introduction

Recent reports on the reductive carbon–oxygen bond cleavage of cyano-substituted anisole radical anions suggested decay by three major pathways, which are dependent on the electron-density distribution of the particular radical–anion isomer.[1] In the case of 2-cyanoanisole, dimerization of the radical anion results in the intermediacy of a dimeric dianion, which undergoes intramolecular electron transfer to produce 2-cyanophenoxide, methide ion, and 2-cyanoanisole. No dimeric-type products were observed either by cyclic voltammetry or analysis of the final products of electrolysis. In contrast to the 2-cyano isomer, the 4-cyanoanisole radical anion undergoes facile carbon–oxygen bond cleavage to form 4-cyanophenoxide and methyl radical.

There are no reports on the reductive electrochemical cleavage of carbon–oxygen bonds in diaryl ethers, including either diphenyl ether or substituted diphenyl ethers. In contrast, there are several reports on the reductive cleavage of diphenyl ether using chemical reductants.[2-10] Recent data by Woolsey and co-workers suggest

(1) Koppang, M. D.; Woolsey, N. F.; Bartak, D. E. *J. Am. Chem. Soc.* **1984**, *106*, 2799.

(2) Stock, L. M. In "Coal Science"; Gorbaty, M. L., Larson, J. W., Wender, I., Eds.; Academic Press: New York, 1982; Vol. 1, pp 169–173, reviews carbon–oxygen bond cleavage pathways in reductive alkylation reactions.

0002-7863/85/1507-4692$01.50/0

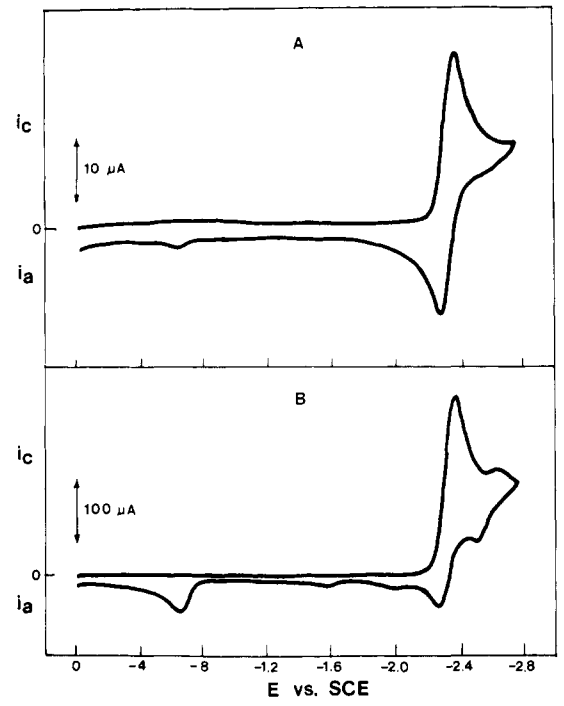

Figure 1. Cyclic voltammograms in 0.2 M TBAP-DMF at a scan rate of 0.1 V s^{-1} (A) 5.2 × 10^{-4} M 4-cyanodiphenyl ether, (B) 5.4 × 10^{-3} M 4-cyanodiphenyl ether. The planar platinum electrode area was 0.20 cm^2.

a unimolecular radical-anion cleavage pathway for diphenyl ether under Na/HMPA/THF conditions to produce a phenyl radical and phenoxide ion.[3] Bunnett and co-workers have demonstrated the intermediacy of phenyl radicals in the reduction of diphenyl ether in K/NH_3.[4,5] Subsequent reactions of the phenyl radicals with nucleophiles, including amide ion and acetone enolate, by the $S_{RN}1$ reaction mechanism were noted.[5,6] Radical-anion cleavage of diphenyl ether to phenoxide ion and a phenyl radical which can be further reduced to a phenyl anion has been proposed by Screttas.[7] Reduction of diphenyl ether solutions with Li/naphthalene/THF[7] and Li/THF[8] followed by carbonation resulted in the formation of significant amounts of 2-carboxydiphenyl ether and benzoic acid in addition to phenol. In contrast to these proposals, there have been reports of the two-electron reduction of diphenyl ether to a dianion, which undergoes carbon-oxygen bond cleavage to directly form a phenyl anion and phenoxide ion.[9,10]

Most of the above literature reports rely solely on product analysis to postulate a mechanism. Kinetic data together with product analysis appear to be necessary to fully elucidate the reaction pathways in carbon-oxygen bond cleavage of diaryl ethers including diphenyl ether. The direct electrochemical reduction of diphenyl ether to its radical anion in aprotic solvents has been recently observed.[11] However, quantitative kinetic data were difficult to obtain because of a very negative reduction potential and the instability of the radical anion. Therefore, substitution of the phenyl ring in diphenyl ether with electron-withdrawing substituents appears to be necessary to obtain quantitative information on aryl carbon-oxygen bond cleavage in diphenyl ethers. Since previous results have indicated that the cyano substituent was capable of controlling reactivity of the radical anion of anisole toward dimerization vs. unimolecular cleavage,[1] the cyano-substituted diphenyl ethers were studied. We report herein on the electrochemical formation and resultant reactions of 2- and 4-cyanodiphenyl ether radical anions. We will demonstrate that these relatively long-lived radical anions react by dimerization pathways with the formation of stable dimeric type products.

Table I. Controlled-Potential Electrolysis[a] of 4-Cyanodiphenyl Ether

initial ether concn, mM	product yields, %						
	n	PhOH	NCPhOH	PhCN	**1**	**3**[b]	**4**[b]
4.8	1.1	46	3	5	31	28	32
49	1.0	50	1	9	33	22	24

[a] The potential was −2.3 V vs. SCE. For details of the electrolysis experiments, see the Experimental Section. [b] Product yields defined as (concn of product × 2/initial concn of substrate) × 100%.

Results and Discussion

4-Cyanodiphenyl Ether (1). 1. Cyclic Voltammetry. The reductive electrochemical behavior of 4-cyanodiphenyl ether (**1**) is illustrated in Figure 1. A single reduction wave at −2.35 V, which has a peak current function ($i_p/v^{1/2}C$) consistent with a one-electron process or radical-anion formation, is noted at relatively low concentrations or high scan rates (Figure 1A). Upon scan reversal, an oxidation wave appears at −2.29 V, which is due to reoxidation of the radical anion back to **1**. The ratio of peak currents (i_{pa}/i_{pc}) for this redox couple is concentration dependent and approaches unity at a scan rate of 0.1 V s^{-1} for an ether concentration of 0.52 mM (Figure 1A).[12] In addition, the ratio of peak currents, a measure of radical-anion stability, decreases with decreasing scan rate. These data indicate disappearance of the radical anion by a process other than unimolecular fragmentation.

Disappearance of the radical anion results in the formation of new waves in the voltammogram (Figure 1B). Oxidation waves at −0.65, −1.57, and −2.01 V and a reversible redox couple with a cathodic peak potential of −2.56 V appear concomitantly with the decrease in the oxidation wave at −2.29 V.[13] Successive cycling with an anodic switching potential of −1.4 V yields reduction waves at −1.63 and −2.07 V, which are respectively coupled to the oxidation waves of −1.57 and −2.01 V. These two reversible redox couples can be assigned to the stepwise reduction of 4,4′-dicyanobiphenyl (**3**) to its radical anion and dianion by comparison to an authentic sample of 4,4′-dicyanobiphenyl. If an anodic switching potential of −0.4 V is employed, the oxidation wave at −0.65 V is completely irreversible for successive cycles. In contrast, the wave at −2.56 V is reversible even at scan rates of 0.01 V s^{-1}. The nature of the species responsible for these waves will be discussed in more detail (vide post).

2. Controlled-Potential Electrolysis. A series of controlled-potential electrolysis experiments was carried out on **1** at an applied potential of −2.3 V vs. SCE (Table I). The potential was selected so as to prevent reduction of the electroactive species (E_{pc} = −2.56 V) which is apparently produced as the result of radical-anion disappearance of **1**. Upon the addition of charge in excess of 1 F mol^{-1}, the potential was stepped back to −1.3 V in order to reoxidize any electroactive products which could have been concurrently reduced during the experiment (e.g., 4,4′-dicyanobiphenyl). After the net addition of 1 F mol^{-1}, approximately 30% of the ether remained. The major oxygen-containing product was phenol, with minor amounts of 4-cyanophenol. Although phenol was a major product of the electrolyses, benzonitrile was found in only minor amounts. Instead, the cyano-substituted phenyl ring was found primarily in the form of two dimeric type products,

(3) Patel, K. M.; Baltisberger, R. J.; Stenberg, V. I.; Woolsey, N. F. *J. Org. Chem.* **1982**, *47*, 4250.
(4) Bard, R. R.; Bunnett, J. F.; Creary, X.; Tremelling, M. J. *J. Am. Chem. Soc.* **1980**, *102*, 2852.
(5) Rossi, R. A.; Bunnett, J. F. *J. Am. Chem. Soc.* **1974**, *96*, 112.
(6) Rossi, R. A.; Bunnett, J. F. *J. Am. Chem. Soc.* **1972**, *94*, 683.
(7) Screttas, C. G. *J. Chem. Soc., Chem.* Commun. **1972**, 869.
(8) Gilman, H.; Dietrich, J. J. *J. Org. Chem.* **1957**, *22*, 851.
(9) Eargle, D. H., Jr. *J. Org. Chem.* **1963**, *28*, 1703.
(10) Eisch, J. J. *J. Org. Chem.* **1963**, *28*, 707.
(11) Koppang, M. D.; Thornton, T. A.; Bartak, D. E., to be submitted for publication.

(12) Peak current ratios were determined according to: Nicholson, R. S. *Anal. Chem.* **1966**, *38*, 1406. The ratios were measured from CV's with a cathodic switching potential of −2.50 V.
(13) In addition, an oxidation wave is observed at 0.1 V (not shown in the figure) at relatively slow scan rates. The height of this wave is of similar magnitude to those assigned to the dimeric products and is relatively prominent after the electrolysis of **1**. Comparison of these data to a sample of potassium phenoxide indicates that the wave represents the oxidation of phenoxide ion.

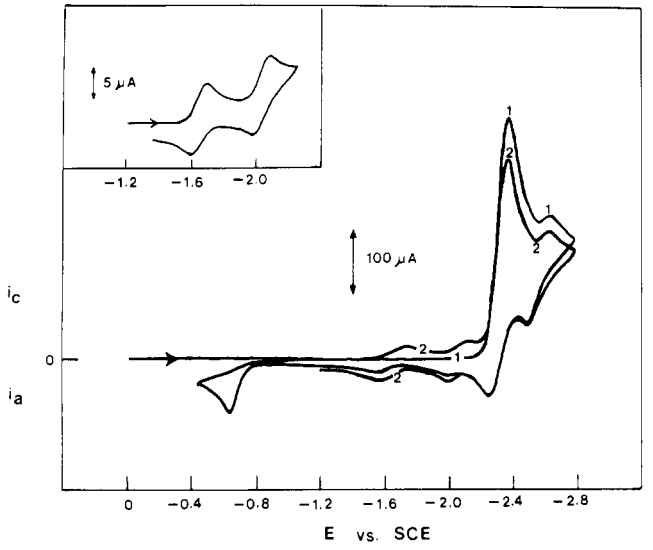

Figure 2. Cyclic voltammogram of 7.4×10^{-3} M 4-cyanodiphenyl ether in 0.2 M TBAP-DMF at a scan rate of 0.1 V s^{-1}. The planar platinum electrode area is 0.20 cm^2. Insert: Cyclic voltammogram of 2,4′-dicyano-5-phenoxybiphenyl (1.4×10^{-4} M) under the above conditions.

4,4-dicyanobiphenyl (**3**) and 2,4′-dicyano-5-phenoxybiphenyl (**4**).

The dimeric type product **4**, which was isolated by preparative gas chromatography from an electrolysis solution, was examined for its electrochemical behavior by cyclic voltammetry (Figure 2 insert). Two reversible reduction waves for **4** with cathodic peak potentials of −1.70 and −2.08 V vs. SCE were observed. Thus, **4** can be reduced to the radical anion and dianion, respectively, at potentials similar to those for 4,4′-dicyanobiphenyl (**3**) (vide ante). This electrochemical behavior is consistent with a dicyanobiphenyl compound with an additional *m*-phenoxy substituent, which should have a marginal effect on its reduction potential. After the determination of the dimeric products of electrolysis, the oxidation wave at −0.65 V was further investigated by cyclic voltammetry (Figure 2). The initial cycle produced a voltammogram similar to that shown in Figure 1. The second cycle, which was initiated at an anodic switching potential of −0.4 V, showed a decrease in the height of the reduction wave at −2.35 V due to normal depletion of **1** in the vicinity of the electrode. In addition, an increase and broadening of the redox couples at −1.7 and −2.1 V were observed. Although 4,4′-dicyanobiphenyl was reduced at similar potentials, the broadening of the waves in the cathodic direction implied the formation of **4** on the second cycle. The formation of **4** was the apparent result of oxidation of a precursor to **4** at −0.65 V. These data are consistent with the behavior displayed during the electrolysis experiments. If the electrolysis solutions were exposed to air upon completion of the experiment, **4** was produced in amounts as shown in Table I. If perchloric acid was added to the solutions after the experiment, the amount of **4** formed was greatly reduced.[14]

3. Kinetics for Disappearance of the Radical Anion of 1 and Formation of Products. Cyclic voltammetric and electrolysis data revealed that the radical anion of **1** is unstable in DMF and reacts by a *concentration-dependent* pathway to eventually yield carbon–oxygen bond cleavage products. Although useful for understanding, these experimental data do not provide a clear mechanistic picture. Double- and single-potential-step chronoamperometry (DPSCA and SPSCA, respectively) were employed to determine the order and rate of disappearance of the radical anion of **1** and formation of products.[15] Initial SPSCA experiments, conducted at an electrode potential sufficiently

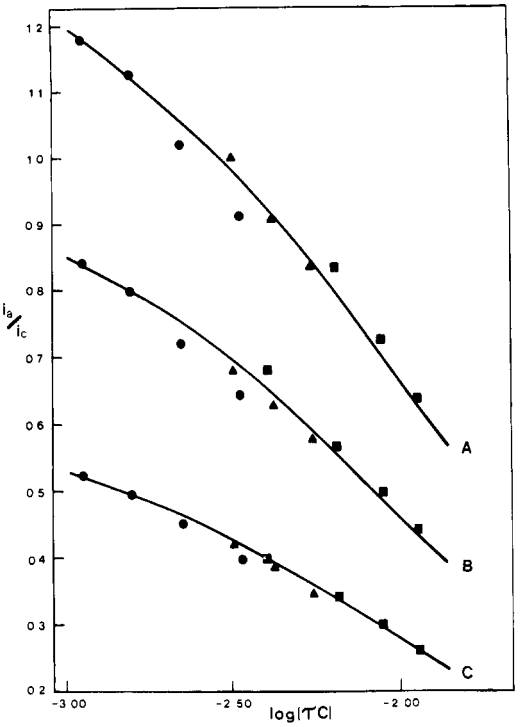

Figure 3. Double-potential-step chronoamperometric data for the disappearance of the 4-cyanodiphenyl ether radical anion in 0.2 M TBAP–DMF. The solid curves were obtained by computer simulation[17] of the processes described by eq 1 and 2 with $k_2 = 1.1 \times 10^2$ M^{-1} s^{-1} for the following ratios of t_a/τ: (A) 0.2, (B) 0.3, and (C) 0.5. The cathodic electrolysis time is designated by τ; the anodic electrolysis time by t_a. The points are the experimental data with 4-cyanodiphenyl ether concentrations: (●) 2.26×10^{-3} M; (▲) 5.43×10^{-3} M; (■) 8.15×10^{-3} M.

negative to reduce the surface concentration of **1** to zero ($E_{applied} = -2.50$ V), yielded results which are consistent with a one-electron, diffusion-controlled process (1 ms < t < 1 s).[16] DPSCA was employed to follow the disappearance of the radical anion of **1**. The radical anion of **1** was generated for a predetermined cathodic electrolysis time τ (τ < 1 s) at −2.50 V; the potential was then stepped back to −2.00 V. Anodic currents (i_a) were measured for anodic electrolysis times (t_a) of 0.2-, 0.3-, and 0.5τ. Ratios of anodic current (i_a) to cathodic current (i_c) measured at τ are a measure of the stability of the radical anion and are presented in Figure 3 as a function of τ and ether concentration (C). These data were compared to a digital simulated working curve[17] for the following reaction sequence:

$$\mathrm{ArOPh} + e^- \rightleftarrows \mathrm{ArOPh}^{-}\cdot \qquad \mathrm{Ar} = \text{4-cyanophenyl} \qquad (1)$$

$$2\mathrm{ArOPh}^{-}\cdot \xrightarrow{k_2} \text{products} \qquad (2)$$

Good agreement between the working curve and the experimental data was obtained with a rate constant of 1.1×10^2 M^{-1} s^{-1}, which suggests that the 4-cyanodiphenyl ether radical anion disappears by an irreversible second-order process.

The cyclic voltammetric data (vide ante) indicate that three reversible redox couples are produced as the result of radical–anion disappearance for **1**. Two of the couples are assigned to the electrochemical behavior of **3**. Thus, two species are apparently produced from the decomposition of the radical anion of **1** and are responsible for the reversible reduction waves. SPSCA was employed for measuring the rate of formation of the reducible

(14) Protonation of electrolysis products by $HClO_4$ under an argon atmosphere resulted in the formation of a compound of molecular weight 298 in addition to compound **4** (MW = 296). Similar behavior was also observed for electrolysis solutions of 2-cyanodiphenyl ether.

(15) Bard, A. J.; Faulkner, L. R. "Electrochemical Methods"; Wiley: New York, 1980; Chapter 5.

(16) The current–time function ($it^{1/2}/C$), which is proportional to the electron stoichiometry, was 33 ± 1 A $s^{1/2}$ mol^{-1} cm^3 on a planar platinum electrode (geometric area, 0.20 cm^2) for t < 1 s. This value can be compared with an $it^{1/2}/C$ value of 37 A $s^{1/2}$ mol^{-1} cm^3, obtained on the same electrode for *m*-tolunitrile, which is reduced via a one-electron, diffusion-controlled process.

(17) Feldberg, S. W. *Electroanal. Chem.* **1969**, *3*, 199.

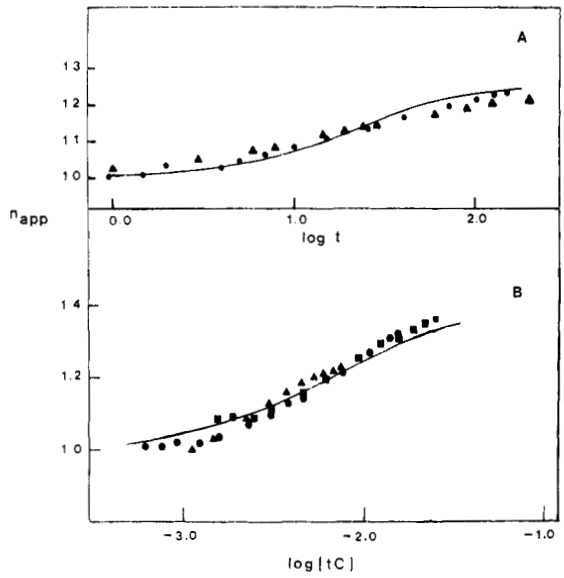

Figure 4. Single-potential-step chronoamperometric data for the change in electron stoichiometry or product formation in the reduction of 4-cyanodiphenyl ether in 0.2 M TBAP-DMF: (A) $E_{app} = -2.43$ V on a planar, shielded platinum electrode (0.28 cm^2); (B) $E_{app} = -2.75$ V on a planar platinum electrode (0.20 cm^2). The solid curves were obtained by computer simulation[17,20] of: (A) eq 5–7 with a first-order rate constant (k_1) of 3.8×10^{-2} s^{-1}; (B) eq 8–12 with a second-order rate constant (k_2) of 9.6×10^{1} M^{-1} s^{-1} and $K_{eq} = 10^{-4}$.[22] The experimental points are for concentrations of 4-cyanodiphenyl ether: (A) (●) 3.74×10^{-3} M, (▲) 1.99×10^{-2} M; (B) (▲) 7.4×10^{-3} M, (●) 1.53×10^{-2} M, (■) 3.06×10^{-2} M.

products by following the change in electron stoichiometry (i.e., $it^{1/2}/C$ was monitored as a function of time and concentration of **1**).

Two potential-step programs were employed for the SPSCA experiments. For the first program (I), the potential of the electrode was stepped to a value sufficiently negative to reduce the surface concentration of **1** to virtually zero ($E = -2.43$ V). However, the potential of the electrode was positive of the reversible reduction wave at −2.56 V (see Figure 1B), but sufficiently negative to allow for the concurrent diffusion-controlled reduction of **3** to its dianion ($E_{pc} = -1.63$ and −2.07 V). A constant $it^{1/2}/C$ value of 49 ± 1 A s$^{1/2}$ mol^{-1} cm^3 (10 ms $< t <$ 1 s) was observed on a shielded platinum electrode (geometric area of 0.28 cm^2). This value can be compared with a value of 55 ± 2 A s$^{1/2}$ mol^{-1} cm^3, which was obtained for *m*-tolunitrile (one-electron process) on the same electrode (10 ms $< t <$ 100 s). For times greater than 1 s, $it^{1/2}/C$ increases monotonically for increasing time owing to the formation and subsequent reduction of **3** to its dianion. Figure 4A is a plot of SPSCA data for **1** employing this potential-step program. The data were normalized with respect to the $it^{1/2}/C$ value obtained for **1** when the reduction of **1** was a diffusion-controlled, one-electron reduction ($t < 1$ s).[18] The value of n_{app} was determined as a function of time (1 s $< t <$ 100 s) and was found to increase to an upper limit of 1.25 *independently* of the concentration of **1**. Since these data indicate that the formation of **3** is significantly slower than the disappearance of the radical anion of **1**, an intermediate species is necessary between the radical anion and the formation of **3** in the reaction channel. Since the radical anion disappears via an irreversible dimerization-type path, a possible intermediate is a dimeric dianion. The formation of a dimeric dianion intermediate, which results from radical–anion dimerization with subsequent slow intramolecular electron transfer, has been postulated in the reduction pathways of 2-fluorobenzonitrile[19] and 2-cyanoanisole.[1] In the latter case, a dimeric dianion decomposes slowly ($k = 2 \times 10^{-2}$ s^{-1}) with carbon–oxygen bond cleavage to form *o*-cyanophenoxide, methide ion, and unreduced substrate. A significant pathway for the radical anion of **1** is therefore dimerization by 4–4 coupling with respect to the cyano substiuent to produce the dimeric dianion **6** (eq 3).

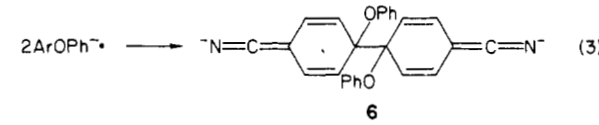

(3)

6

The resultant dimeric dianion subsequently undergoes a relatively slow carbon–oxygen bond cleavage to yield phenoxide and **3** (eq 4). The increase in the n_{app} to a value of 1.25 for the formation

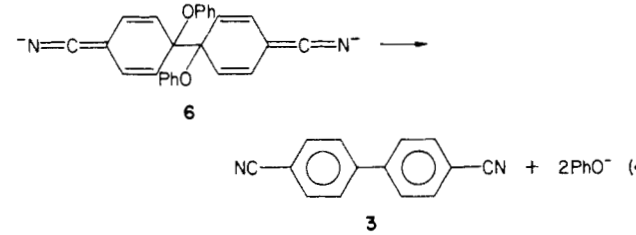

(4)

6 **3**

of **3** indicates that 25% of **1** follows this reaction channel, which is in reasonable agreement with the electrolysis product analysis (Table I).

Since the rate of disappearance of the radical anion of **1** is much more rapid than the appearance of **3**, the reaction sequence was digitally simulated as eq 5–7.[20] The resultant working curve is

$$8\text{ArOPh} + 8e^- \xrightarrow{\text{rapid}} (\text{ArOPh})_2^{2-} + \text{products} \quad (5)$$

$$(\text{ArOPh})_2^{2-} \xrightarrow[\text{slow}]{k_1} (\text{Ar})_2 + 2\text{PhO}^- \quad (6)$$

$$(\text{Ar})_2 + 2e^- \rightleftharpoons (\text{Ar})_2^{2-} \quad (7)$$

the solid line in Figure 4A. A good fit was obtained for these data with the working curve for a rate constant (k_1) of 3.8×10^{-2} s^{-1}.

A second potential-step program (II) was also employed for the SPSCA experiments. The potential of the planar platinum electrode (geometric area, 0.20 cm^2) was changed from a value of −2.10 to −2.75 V, which was sufficiently negative to cause the diffusion-controlled reductions of **1** and the electroactive product with $E_{pc} = -2.56$ V (see Figure 2). Although 4,4′-dicyanobiphenyl (**3**) can be reduced at this potential, complications due to concurrent reduction of **3** were prevented by imposing the time limit of $t < 1$ s for the SPSCA experiment. A constant $it^{1/2}/C$ value of 33 ± 1 A s$^{1/2}$ mol^{-1} cm^3 was observed for $t < 50$ ms.[16] However, kinetic control in the formation of the electroactive species was noted by an increasing $it^{1/2}/C$ with increasing time at $t > 50$ ms. In contrast to the behavior observed for the SPSCA experiments using the potential program I, the $it^{1/2}/C$ values were observed to increase with increasing concentration of **1**. These $it^{1/2}/C$ values were again normalized as n_{app} with respect to the one-electron $it^{1/2}/C$ value for **1** obtained on this same electrode. Figure 4B is a summary of the SPSCA data (program II) in which the change in n_{app} was determined as a function of time ($t < 1$ s) and concentration of **1**.

The DPSCA data suggest that the radical anion of **1** disappears by a second-order pathway. The appearance of products, however, suggests at least two reaction pathways. One of the pathways, accounting for 25% of the disappearance of **1**, involves a 4–4 dimeric coupling to eventually yield **3**. Since a second dimeric type product, 2,4′-dicyano-5-phenoxybiphenyl (**4**), is also produced,

(18) The SPSCA data ($it^{1/2}/C$) were normalized such that the apparent electron stoichiometry (n_{app}) = ($it^{1/2}/C$)/(49 A s$^{1/2}$ mol^{-1} cm^3). The value of 49 A s$^{1/2}$ mol^{-1} cm^3 represents the $it^{1/2}/C$ value for the diffusion-controlled one-electron reduction of 4-cyanodiphenyl ether for this shielded electrode as described earlier in the text.

(19) Houser, K. J.; Bartak, D. E.; Hawley, M. D. *J. Am. Chem. Soc.* **1973**, *95*, 6033.

(20) This simulation sequence has been previously applied[1,19] for dimeric dianion intermediates undergoing *slow* decomposition. Although Evans et al.[21] report a closed-form solution of a similar problem, occurrence of other reaction pathways for loss of radical anion of **1** prompted the use of simulation techniques for the problem.

(21) Evans, D. H.; Rosanke, T. W.; Jimenez, P. J. *J. Electroanal. Chem.* **1974**, *51*, 449.

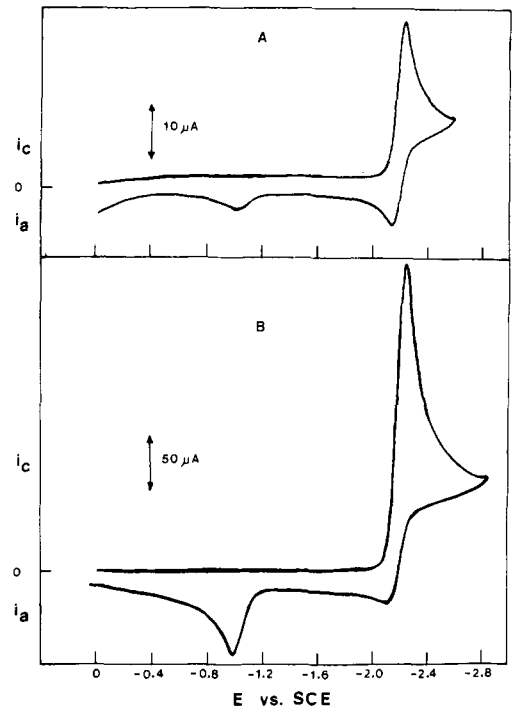

Figure 5. Cyclic voltammograms of (A) 5.2×10^{-4} M, (B) 5.4×10^{-3} M 2-cyanodiphenyl ether in 0.2 M TBAP-DMF (conditions same as Figure 1).

a second major pathway for the second-order disappearance of the radical anion can result in the formation of a 2–4 coupled dimeric dianion **7** (eq 8 and 9).

$$\mathrm{ArOPh} + e^- \rightleftarrows [\mathrm{ArOPh}]^{-\cdot} \qquad \mathrm{Ar} = \text{4-cyanophenyl} \quad (8)$$

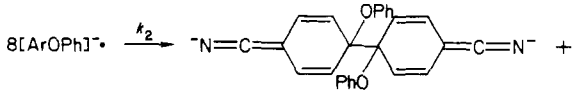

6

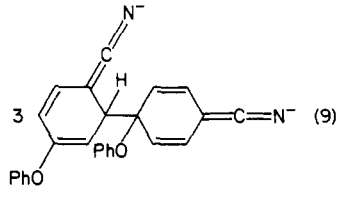

(9)

7

The 2–4 dimeric dianion **7** cannot be completely rearomatized by loss of two phenoxide ions but can lose one phenoxide ion (eq 10 to regain part of its aromatic stabilization energy. The latter

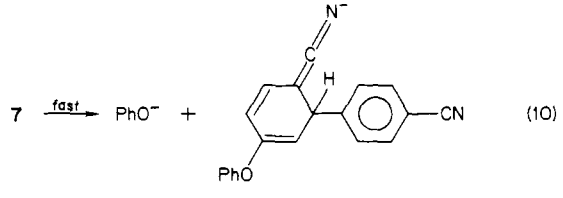

(10)

8

loss of phenoxide ion yields the anion **8** which can exist in one of two possible tautomeric forms. The reduction potential and the reversible nature of the wave at −2.56 V are consistent with an ionic species **8**, which should undergo a reversible one-electron reduction:

$$8 + e^- \underset{}{\overset{E_{pc} = -2.56\ \mathrm{V}}{\rightleftarrows}} 8^{-\cdot} \quad (11)$$

A reaction mechanism consistent with eq 8–11 was computer simulated with the inclusion of the homogeneous electron-transfer nuance (eq 12) with a $K_{eq} = 1 \times 10^{-4}$, which was based on the

$$1^{-\cdot} + 8 \overset{K_{eq}}{\rightleftarrows} 8^{-\cdot} + 1 \quad (12)$$

redox potentials of **1** and the new electroactive product **8** (E_{pc} = −2.56 V).[22] The solid line (Figure 4B) represents the simulated working curve of an SPSCA experiment. A good fit was obtained for a rate constant (k_2) of 9.6×10^1 M^{-1} s^{-1}. Thus, the rate of formation of the reducible species at −2.56 V is consistent with the radical-anion dimerization reaction acting as the rate-controlling step in the formation of **8**.

Potential-step program II was also applied to a shielded electrode (geometric area of electrode, 0.28 cm^2). The electron stoichiometry or n_{app} was observed to increase from a value of 1.0 to a limiting value of 1.62 ($t < 100$ s). The change in n_{app} as a function of time on the shielded electrode consists essentially of two parts. For shorter times ($t < 1$ s, concentration of **1** > 3 mM), n_{app} increases from 1.0 to 1.38 as a function of time and concentration of **1**. At longer times ($t > 1$ s) n_{app} increases from 1.38 to 1.62 independently of concentration of **1**. These data are in agreement with the results and conclusions obtained in the previously described SPSCA experiments.

Oxidation of the proposed intermediate anion **8** by the loss of $2e^-$ and a H^+ will yield the observed electrolysis product **4** (eq 13). The observation for the formation of **4** as a result of the

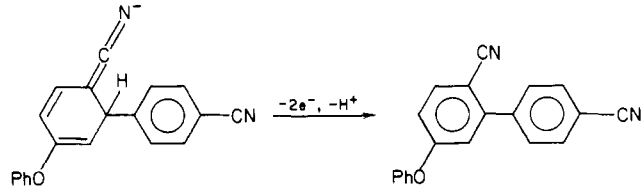

8 **4**

(13)

cyclic voltammetric oxidation process at −0.65 V (see Figure 2) suggests that oxidation of anion **8** occurs at −0.65 V. Thus, these data indicate that the dimeric anion **8** can be reversibly reduced to a radical dianion at E_p = −2.56 V (eq 11) as well as irreversibly oxidized at −0.65 V to 2,4′-dicyano-5-phenoxybiphenyl (**4**).

2-Cyanodiphenyl Ether. 1. Cyclic Voltammetry. The cyclic voltammetric behavior of 2-cyanodiphenyl ether (**2**) is markedly dependent on the concentration of **2**. As the concentration of **2** is increased from 0.52 to 5.4 mM (Figure 5), the peak current ratio (i_{pa}/i_{pc}) for the radical-anion redox couple for **2** (E_{pc} = −2.22 V, E_{pa} = −2.14 V) decreases. In addition, the peak current ratio decreases with decrasing scan rate. Concurrent with the ratio decrease are the appearance and increase in magnitude of an oxidation wave at −1.02 V, which exhibits irreversible behavior. These data suggest that the radical anion of **2** disappears by a concentration-dependent pathway resulting in the formation of an oxidizable species (E_{pa} = −1.02 V).

Although the current ratio for the radical anion of **2** decreases with decreasing scan rate, the ratio begins to increase for very slow scan rates (<0.05 V s^{-1}). This voltammetric behavior is considered a diagnostic criterion[23,24] for a reversible follow-up chemical reaction of an electrochemically generated species such as a radical anion. In addition, this type of cyclic voltammetric behavior has been recently reported for the reduction of 9-cyanoanthracene,[23] which undergoes reversible dimerization.

2. Controlled-Potential Electrolysis. A series of controlled-potential electrolysis experiments was carried out for **2** at an applied potential of −2.2 V vs. SCE (Table II). The reductive decomposition of **2** involves primarily carbon–oxygen bond cleavage resulting in products and distributions similar to those observed for 4-cyanodiphenyl ether (**1**) (vide ante). Electrolysis

(22) Hawley, M. D.; Feldberg, S. W. *J. Phys. Chem.* **1966**, *70*, 3459.
(23) (a) Yildiz, A.; Baumgartel, H. *Ber. Bunsenges. Phys. Chem.* **1977**, *81*, 1177. (b) Hammerich, O.; Parker, V. D. *Acta Chem. Scand., Ser. B* **1981**, *35*, 341. (c) Amatore, C.; Pinson, J.; Saveant, J. M. *J. Electroanal. Chem.* **1982**, *137*, 143.
(24) Evans, D. H.; Jimenez, P. J.; Kelly, M. J. *J. Electroanal. Chem.* **1984**, *163*, 145.

Table II. Controlled-Potential Electrolysis[a] of 2-Cyanodiphenyl Ether

initial ether concn, mM	n	product yields, % PhOH	NCPhOH	PhCN	**2**	PhOPh	**5**[b]
11	1.3	28	3	7	55	11	20
47	1.2	29	6	7	42	5	14
22	1.5	36	4	7	32	7	22

[a] The potential was −2.2 V vs. SCE. For details of the electrolysis experiments, see the Experimental Section. [b] Product yields defined as (concn of product × 2/initial concn of substrate) × 100%.

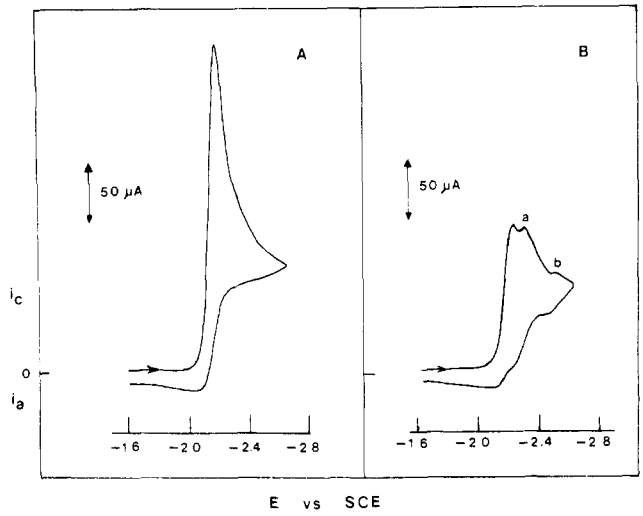

Figure 6. Cyclic voltammograms of 4.7×10^{-2} M 2-cyanodiphenyl ether in 0.2 M TBAP-DMF: (A) before electrolysis and (B) after electrolysis at $E_{app} = -2.25$ V with the addition of 1.2 F mol^{-1}. The scan rate was 0.1 V s^{-1} on a platinum-bead electrode.

of **2** also results in formation of a dimeric type product, 2′,4-dicyano-3-phenoxybiphenyl (**5**). A minor reaction pathway for **2** involves a carbon–carbon bond cleavage with loss of a cyano substituent to yield diphenyl ether. The dimeric-type product, 2,2′-dicyanobiphenyl, is not observed as an electrolysis product.

Cyclic voltammetry was utilized to study the electroactive species which are produced during the electrolysis (Figure 6). A voltammogram recorded before the electrolysis (A) is similar to those discussed previously (see Figure 5); the oxidation wave at −1.02 V (not shown) is the only observable redox process in addition to the reduction wave of **2**. A voltammogram recorded after the electrolysis experiment (B) shows the presence of new electroactive species by the appearance of two new reduction couples (a and b) with cathodic peak potentials of −2.32 and −2.54 V. The first couple (a) can be assigned to the reduction of benzonitrile. The latter (b) appears at a potential similar to the potential of the wave in the CV of 4-cyanodiphenyl ether (see Figure 1B), proposed to occur as the result of an anion precursor (**8**) to 2,4′-dicyano-5-phenoxybiphenyl (**4**). Therefore, wave b is probably due to the reduction of an dimeric anion, which can also be oxidized to the electrolysis product, 2′-4-dicyano-3-phenoxybiphenyl (**5**). The formation of the two reducible products from the decomposition of the radical anion of **2** is *much slower* than the initial radical-anion disappearance. This is in sharp contrast to the rate of formation of the oxidizable species ($E_{pa} = -1.02$ V) which is produced concomitantly with radical-anion disappearance.

3. Kinetics for the Radical-Anion Disappearance and Reaction Pathway. The kinetics for the disappearance of the radical anion of **2** was studied by SPSCA and DPSCA techniques. For the SPSCA experiments, the potential of a shielded platinum electrode (geometric area = 0.95 cm^2) was changed from −1.95 to −2.68 V vs. SCE. The $it^{1/2}/C$ value remained relatively constant (130 ± 5 A $s^{1/2}$ mol^{-1} cm^3) for 100 ms < t < 150 s (concn of **2** = 3.5 mM). This value can be compared with the value of 160 ± 10 A $s^{1/2}$ mol^{-1} cm^3 for *m*-tolunitrile, which was obtained on the same electrode over a similar time window. Thus, benzonitrile or the reducible species ($E_{pc} = -2.54$ V) observed in the voltammograms (cf. Figure 6, vide ante) is not produced to any significant amount for times up to 150 s.

DPSCA was employed to follow the disappearance of the radical anion of **2**. For these experiments, the electrode potential was changed from −1.95 to −2.45 V vs. SCE. After cathodic electrolysis time τ, the potential was stepped back to −1.95 V. The ratio of anodic current to cathodic current was again measured for various ratios of anodic electrolysis time (t_a) to cathodic electrolysis time (τ). The current ratios are presented in Figure 7 as a function of τ and substrate concentration (C). These data clearly show that the radical-anion stability decreases with increasing time (τ) and concentration of **2**. However, the current ratios attain a minimum value, which is subsequently followed by an increase with increasing log (τC). This behavior, which is analogous to the results from the voltammetric studies, suggests that the radical anion disappears by a reversible, concentration-dependent pathway. A mechanism consistent with these data is a reversible radical-anion dimerization:

$$\mathrm{ArOPh} + e^- \rightleftarrows [\mathrm{ArOPh}]^{-\cdot} \qquad \mathrm{Ar} = \text{2-cyanophenyl} \qquad (14)$$

$$2[\mathrm{ArOPh}]^{-\cdot} \underset{k_b}{\overset{k_f}{\rightleftharpoons}} [\mathrm{ArOPh}]_2^{2-} \qquad (15)$$

The solid lines in Figure 7 represent digitial simulation of eq 14 and 15. Good agreement was obtained for the forward and backward rate constants from the simulated working curves with substrate concentations of 1.44, 5.39, and 13.5 mM. From these results, we propose that the radical anion of **2** undergoes a reversible dimerization (eq 14 and 15) with a forward rate constant (k_f) of (1.17 ± 0.06) × 10^3 M^{-1} s^{-1} and a backward rate constant (k_b) of (9.5 ± 0.1) × 10^{-2} s^{-1}.

The product of dimerization, a dianion, which is resistant toward further reduction, should readily undergo oxidation. Dianions produced by dimerization of substituted anthracenes are observed to undergo oxidation at potentials 500–1000 mV more positive than the reduction of substrate.[23a,b] The wave at −1.02 V in the voltammogram of **2** (Figure 5) is consistent with oxidation of a dimeric dianion of **2**.

The radical anion of **2** should couple at carbon sites of highest unpaired electron density. ESR spectroscopy is especially suited for measuring electron densities for various radical anions.[25] Although the radical anion of **2** reacts rapidly, the reversible nature of the reaction allowed for a finite concentration of the radical anion to be detected in the ESR cavity. The radical anion was electrochemically generated in the cavity by controlled-potential electrolysis. The spectrum obtained consists of 46 lines. If the unpaired electron density is localized on the cyano-substituted phenyl ring, a 48-line spectrum should be obtained. Analysis of the spectrum revealed that it consists of a triplet, doublet, doublet, doublet, and doublet with splitting constants of 2.17, 8.77, 4.71, 0.88, and 0.17 G, respectively. A simulation of a spectrum with these constants yielded 46 lines due to four lines overlapping into two and was in good agreement with the experimental spectrum. The triplet of 2.17 G can unequivocally be assigned to the nitrogen. The doublets were assigned on the basis of previously reported assignments for the radical anion of benzonitrile:[25] C(3) = 0.88 G, C(4) = 8.77 G, C(5) = 0.17 G, and C(6) = 4.71 G. From the splitting constants it is reasonable to propose that the dimeric dianion of **2** is the result of predominant 4–4 coupling relative to the cyano-substituted carbon to form dimeric dianion **9**. The

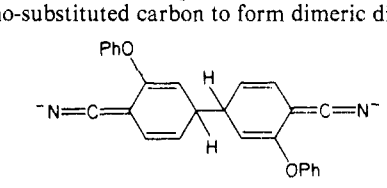

9

dimeric dianion (**9**) should undergo oxidation at a potential of

(25) Rieger, P. H.; Bernal, I.; Reinmuth, W. H.; Fraenkel, G. K. *J. Am. Chem. Soc.* **1963**, *85*, 683.

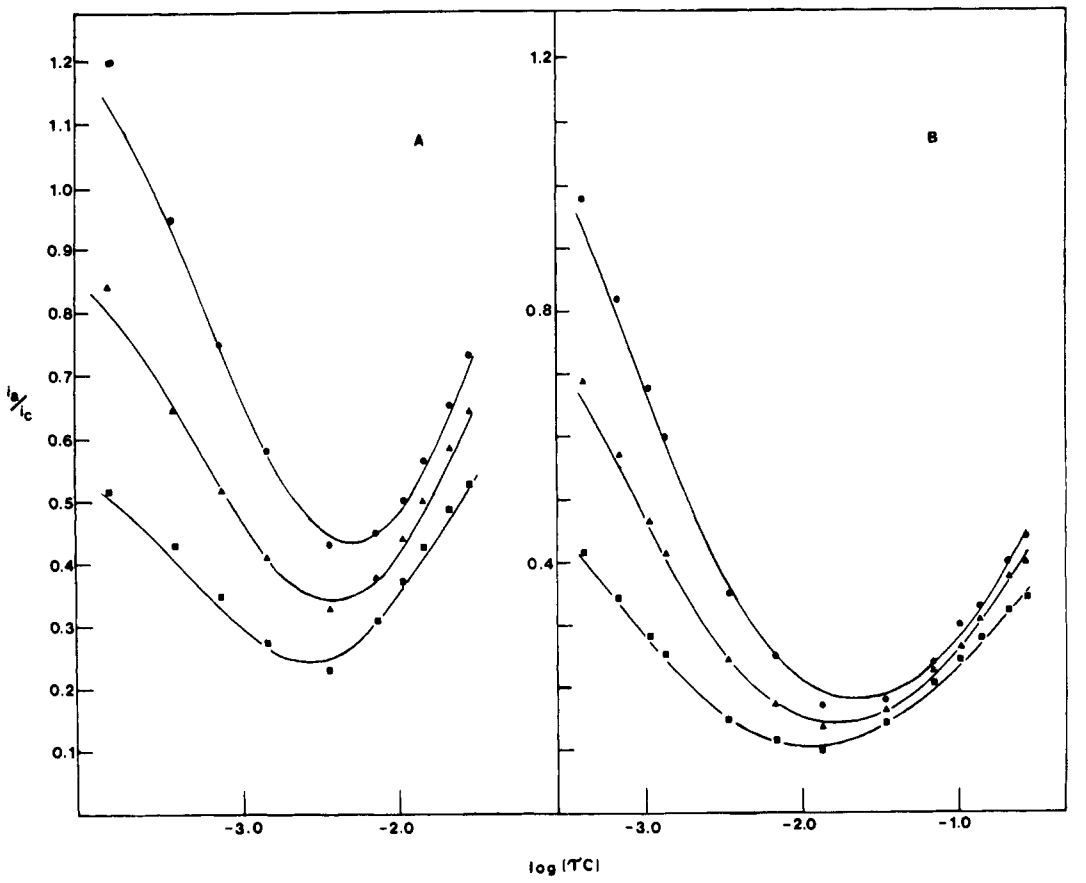

Figure 7. Double-potential-step chronoamperometric data for the disappearance of the 2-cyanodiphenyl ether radical anion in 0.2 M TBAP–DMF. The solid curves were obtained by computer simulation[17] of the processes described by eq 14 and 15 with (A) $k_f = 1.2 \times 10^3$ M^{-1} s^{-1} and $k_b = 1.0 \times 10^{-1}$ s^{-1} at 1.44×10^{-3} M **2** and (B) $k_f = 1.1 \times 10^3$ M^{-1} s^{-1} and $k_b = 9.2 \times 10^{-2}$ s^{-1} at 1.35×10^{-2} M **2**. The ratios of t_a/τ were: (●) 0.2; (▲) 0.3; (■) 0.5, where τ = cathodic electrolysis time and t_a = anodic electrolysis time.

approximately −1.0 V, which is consistent with the oxidation wave observed in Figure 5.

Coupling at both the 4–4 and 4–6 positions should yield relatively stable dianion intermediates which are resistant to further reaction. However, formation of the electrolysis dimeric product **5** can arise only from a 2–4 coupling, with subsequent carbon–oxygen bond cleavage yielding the dimeric anion **10** (eq 16). This

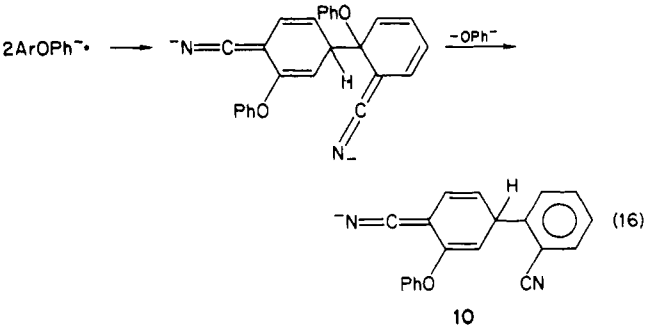

(16)

10

dimeric pathway is apparently much slower because the 2–4 coupled product should undergo relatively fast carbon–oxygen bond cleavage to yield the dimeric anion **10**, which is electroactive (see wave b in Figure 6). Subsequently **10** undergoes oxidation upon workup to produce 2′,4-dicyano-3-phenoxybiphenyl (**5**) (eq 17).

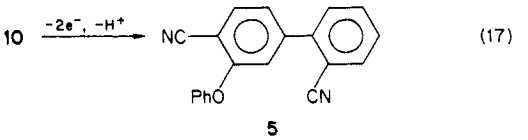

(17)

5

Likewise, other electrolysis products are apparently produced by slower reaction pathways relative to the reversible dimerization pathway.

Summary

The relative instability of dimeric dianion **7** compared with dimeric dianion **6** toward further decomposition (eq 4, 10) requires further comment. The instability of **7** toward carbon–oxygen bond cleavage may be due in part to through-space electronic interactions between the electron-rich cyano substituent and the π framework of the adjacent ring. Electronic repulsions should lead to an increase in the rate of expulsion of the phenoxide leaving group. These interactions can be effectively minimized for **6**. From kinetic studies, the formation of **7** compared to **6** is favored by 3:1. However, the final electrolysis products from **6** and **7** (4,4′-dicyanobiphenyl and 2,4′-dicyano-5-phenoxybiphenyl, respectively) are found in approximately equimolar amounts. Although voltammetric and chronoamperometric studies indicate that conversion of the dimeric anion intermediate **8** to 2,4′-dicyano-5-phenoxybiphenyl is slow (vide ante), decomposition of **8** may occur during the long-time electrolysis experiments. Decomposition of **8** to yield 4-cyanodiphenyl ether and cyanophenyl anion followed by proton abstraction can result in the formation of benzonitrile.

The predominant pathway for radical–anion coupling of 2-cyanodiphenyl ether should involve formation of the sterically unhindered 4–4 coupled dimeric dianion **9**. Coupling in this manner is expected on the basis of our ESR data (vide ante) and is in accordance with previous ESR data[25] and theoretical calculations[26] of electron-density distributions in cyano-substituted aromatic radical anions. The carbons involved in bond formation are not substituted with a suitable leaving group for rearomatization. In addition, decomposition of **9** by an intramolecular electron transfer with subsequent β-type carbon–oxygen bond

(26) (a) Schug, J. C.; Brown, T. H.; Karplus, M. *J. Chem. Phys.* **1962**, *37*, 330. (b) Rieger, P. H.; Fraenkel, G. K. *Ibid.* **1962**, *37*, 2795. (c) Birch, A. J.; Hinde, A. L.; Radom, L. *J. Am. Chem. Soc.* **1980**, *102*, 3370.

cleavage is apparently a restricted pathway on the basis of low yields of 2-cyanophenol (Table II). The resistance of dianion **9** toward further chemical reaction permits the dissociation of **9** to be observed and the rate constant measured (k_b).

Overall resistance of 2-cyanodiphenyl ether toward carbon–oxygen bond cleavage compared to 4-cyanodiphenyl ether is demonstrated by the existence of the competing carbon–carbon bond cleavage pathway to form diphenyl ether. A similar carbon–carbon bond cleavage competes with carbon–oxygen bond cleavage in the reduction of 3-cyanoanisole.[1] The carbon–carbon bond cleavage may be due to protonation of the radical anion of 2-cyanodiphenyl ether, followed by further reduction and elimination in a manner analogous to the reported reductive behavior of benzonitrile.[27] However, the proton availability (electrolyte via a Hoffman elimination or trace water) should be small owing to extensive solvent purification and should cause this pathway to be relatively minor.

We have shown that 4-cyano- and 2-cyanodiphenyl ether both undergo carbon–oxygen bond cleavage under reductive conditions. However, bond cleavage for both isomers is preceded by bond formation via radical–anion dimerization reactions. Dimerization reactions such as these may prove deleterious in the application of reductive conditions for ether cleavage in coal and coal-derived materials. These substances contain aryl moieties capable of stabilizing the resultant radical anions which could allow dimerization reactions to occur. Present work investigating reductive cleavage of polycyclic diaryl ethers is underway and will be reported in the future.

Experimental Section

Instrumentation. Cyclic voltammetric, chronoamperometric, and controlled-potential electrolysis experiments were carried out with a PAR Model 173 potentiostat equipped with a Model 179 digital coulometer. Cyclic voltammetric waveforms were generated by using a digital-controlled, multifunction generator[28] coupled with the PAR 173. Cyclic voltammetric data were recorded on a Soltec X-Y recorder. Potential control and data acquisition for single- and double-potential-step chronoamperometry were performed with an Apple II (64K) microcomputer, which was interfaced with the PAR 173 potentiostat and the PAR 179 current-to-voltage converter output. Data acquisition at the 1-ms time level was achieved with this instrument arrangement.[29] Output from the potentiostat during long-time single-potential-step experiments ($t > 1$ s) was fed through an Ithaco Model 4213 electronic filter operated in the low-band pass mode. All electrochemical measurements were made with positive-feedback electronic compensation for ohmic potential loss. ESR spectra were obtained with a Bruker ER-420 dual-cavity spectrometer. Radical anions of **2** were generated in the microwave cavity with a Scanco electrolytic cell. IR spectra were obtained on a Nicolet MX-S FT-IR. ^{1}H and ^{13}C NMR spectra were obtained with a Varian XL-200 NMR spectrometer. All chemical shifts measured and reported herein are with respect to Me_4Si (δ 0 ppm).

Chemicals. 4-Cyanodiphenyl ether was prepared by a modified Ullman coupling reaction of 4-bromobenzonitrile (Aldrich) and potassium phenoxide according to the method by Tomita and Sato.[30] Purification by vacuum distillation yielded the ether (mp 44–45 °C, lit.[31] mp 43–45 °C) which exhibits the following: IR (CCl_4) 2240 (C≡N), 1250 cm^{-1} (C–O–C) (lit.[32] 2231 and 1260 cm^{-1}); ^{1}H NMR (CD_2Cl_2) δ 6.90–7.70 (m); ^{13}C NMR ($CDCl_3$) δ 105.8 (*C*—C≡N), 118.8 (C≡N), 117.9, 120.4, 125.1 130.2, 134.1, 154.8, and 161.6 (ethereal carbons).

2-Cyanodiphenyl ether was prepared in the following manner. 2-Phenoxybenzoic acid (Aldrich) was converted to the acid chloride with refluxing $SOCl_2$. The acid chloride solution was added slowly to cold ammonium hydroxide to yield the amide. Dehydration of the isolated amide (mp 129–131 °C, lit.[33] mp 131 °C) was accomplished with excess triphenylphosphine and CCl_4 in THF at 50–55 °C.[34] Crude product was vacuum distilled to yield **2** (bp 142 °C (3 mm), lit.[35] bp 188 °C (14 mm), lit.[32] bp 150–154 °C (6 mm)) which exhibits the following: IR (neat) 2250 (C≡N), 1250 cm^{-1} (C–O–C) (lit.[32] 2230 and 1245 cm^{-1}); ^{1}H NMR (CD_2Cl_2) δ 6.84–7.74 (m); ^{13}C NMR ($CDCl_3$) δ 103.5 (*C*—C≡N), 115.9 (C≡N), 116.9, 120.1, 122.7, 124.8, 130.0, 133.7, 134.1, 155.0, and 159.8 (ethereal carbons). Both **1** and **2** were checked for purity by gas chromatographic and high-pressure liquid chromatographic techniques.

Electrochemical grade tetra-*n*-butylammonium perchlorate (TBAP) (Southwestern Analytical Chemicals) was used as the supporting electrolyte. Spectroscopic grade *N*,*N*-dimethylformamide (DMF) (Burdick and Jackson) was employed as the electrochemical solvent. DMF solutions of 0.2 M TBAP were dried by passage through a column containing freshly activated, anhydrous alumina (Woelm W200 neutral grade Super I) in a Vacuum Atmospheres HE-43-2 Dri-Lab glovebox equipped with a HE-493 Dri-Train. The DMF–TBAP solutions were transferred to an all-glass vacuum line and subsequently degassed by several freeze–pump–thaw cycles. Dry, deoxygenated DMF–TBAP solutions[36] were then stored in the glovebox prior to use.

Electrodes and Cells. Solvent and electroactive chemicals were introduced into air-tight, all-glass, electrochemical cells in the glovebox. The electrochemical cells for cyclic voltammetry, chronoamperometry, and controlled-potential electrolysis have been previously described.[37]

The working electrode for cyclic voltammetric and chronoamperometric experiments was a modified Beckman platinum button electrode (no. 39273) with a geometric area of approximately 0.20 cm^2. Long-time chronoamperometric studies ($t > 5$ s) were performed on platinum electrodes (geometric areas of approximately 0.28 and 0.95 cm^2) which were modified by the addition of a 6-mm glass mantle to minimize the effect of edge diffusion.[38] Control experiments on these "shielded" electrodes using *m*-tolunitrile as the electroactive species indicated that chronoamperometric $it^{1/2}$ values are diffusion controlled for $t < 500$ s. The reference electrode was a saturated calomel electrode (SCE) isolated from the working and auxiliary electrodes by means of a glass frit and bridge containing 0.2 M TBAP–DMF. All potential measurements reported herein are with respect to the SCE.

Controlled-Potential Electrolysis and Product Analysis. Controlled-potential electrolyses of **1** and **2** were conducted in the following manner. Solutions of **1** and **2** were reduced at potentials of −2.3 and −2.2 V, respectively. Upon termination of the electrolysis, the potential was stepped back to −1.3 and −1.7 V for **1** and **2**, respectively, in order to reoxidize any electroactive products which could have been concurrently reduced during the experiment. The *n* values (see Tables I and II) represent the net F mol^{-1}, which were consumed. The solutions were then treated as follows for qualitative product analysis. Electrolyzed solution (10 mL) was added to diethyl ether (20 mL) and water (20 mL). The aqueous and organic layers were filtered, acidified (5% HCl, pH <2 for aqueous phase), and separated. The aqueous phase was extracted with diethyl ether (3 × 5 mL) and all organic extracts were combined and dried ($MgSO_4$). The extracted solutions were analyzed by gas chromatography (Varian Aerograph Series 2100 equipped with $^1/_8$-in, all-glass OV-17 columns) and gas chromatography–mass spectroscopy (Hewlett-Packard Model 5875B). Quantitative analysis was accomplished by high-pressure liquid chromatography on a Waters Associates 6000A HPLC equipped with a Model 660 solvent programmer. The electrolyzed solutions were directly injected onto a 0.25 in × 25 cm Alltech C18 column with a 10-μm mean particle size packing. Mobile-phase composition (acetonitrile/4% acetic acid in water) was varied by use of the solvent programmer. Calibration curves were prepared daily and employed for product quantitation. Extracted solutions yielded qualitatively identical HPLC chromatograms compared with chromatograms produced by directly injecting the original electrolysis solutions.

Products **4** and **5** were isolated from extracted electrolysis solutions of **1** and **2**, respectively, by gas chromatography (Varian Aerograph Model 1400, $^1/_4$-in. OV-17 or SE-30 columns, TC detector). An isolated sample of **4** exhibits the following: mass spectrum[39] (GC–MS) *m*/*z* (rel intensity) 296 (M^+, 100), 268 (9), 267 (9), 240 (5), 77 (23), and 51 (10);

(27) Romanin, A. M.; Gennaro, A.; Vianello, E. *J. Electroanal. Chem.* **1978**, *88*, 175.
(28) Bartak, D. E.; Hundley, H. K.; Van Swaay, M.; Hawley, M. D. *Chem. Instrum.* **1972**, *4*, 1.
(29) For further experimental details, see ref 1.
(30) Tomita, M.; Sato, T. *Yakugaku Zasshi* **1957**, *77*, 1024; *Chem. Abstr.* **1958**, *52*, 3719b. Reduction of 4-cyanodiphenyl ether in Na/NH_3 yielded approximately 30% benzonitrile for these authors.
(31) Ashley, J. N.; Barber, H. J.; Ewins, A. J.; Newbery, G.; Self, A. D. H. *J. Chem. Soc.* **1942**, 103.
(32) Suvorov, B. V.; Vorob'ev, P. B.; Bukeikhanov, N. R. *J. Org. Chem. USSR* (*Engl. Transl.*) **1980**, *16*, 556; *Zh. Org. Khim.* **1980**, *16*, 636.
(33) Arbenz, C. *Justus Liebigs Ann Chem.* **1890**, *257*, 76.
(34) Yamato, E.; Sugasawa, S. *Tetrahedron Lett.* **1970**, 4383.
(35) Suter, C. M. *J. Am. Chem. Soc.* **1929**, *51*, 2581.
(36) For further experimental details on solvent–electrolyte purification procedures, see ref 1.
(37) Gores, G. J.; Koeppe, C. E.; Bartak, D. E. *J. Org. Chem.* **1979**, *44*, 380.
(38) We thank Professors E. K. Miller (University of Minnesota) and M. D. Hawley (Kansas State University) for gifts of these electrodes.
(39) Loss of 28 (M − CO) and 29 (M − HCO) mass unit fragments has been shown to be characteristic of diphenyl ether fragmentation; see: Budzikiewicz, H.; Djerassi, C.; Williams, D. H. "Mass Spectrometry of Organic Compounds"; Holden-Day: San Francisco, 1967; Chapter 6, p 249.

IR ($CHCl_3$, solvent-subtracted spectrum) 3025, 2230 (C≡N), 1590, 1480, 1225 cm^{-1} (C-O-C); ^1H NMR (CD_2Cl_2) δ 6.80-7.80 (m); ^{13}C NMR ($CDCl_3$) δ 104.6 and 112.9 (C—C≡N), 118.1 and 118.3 (C≡N), 117.2, 118.5, 120.5, 125.5, 129.5, 130.4, 132.6, and 135.9 (aromatic C-H), 142.1 and 145.6 (biphenyl carbons), 154.5 and 161.8 (ethereal carbons). HRMS:[40] calcd for $C_{20}H_{12}N_2O$, 296.0951, obsd 296.0935; rel intensity calcd for M + 1 22.6, obsd 22.9. An isolated sample of **5** exhibits the following: mass spectrum[39] (GC-MS) *m/z* (rel intensity) 296 (M^+, 100), 297 (M + 1, 23), 295 (24), 268 (14), 267 (20), 164 (10), 77 (26), and 51 (12); IR (CCl_4) 2230 (C≡N), 1551, 1223 cm^{-1} (C-O-C); ^1H NMR (CD_2Cl_2) δ 7.02-7.85 (m); ^{13}C NMR ($CDCl_3$) δ 103.6 and 111.1 (C—C≡N), 115.6 and 117.0 (C≡N), 117.8, 120.3, 123.0, 125.4, 128.8, 129.7, 130.3, 133.0, 133.9, and 134.3 (aromatic C-H), 143.0 and 143.9 (biphenyl carbons), 154.4 and 159.7 (ethereal carbons). Isolated samples of **4** and **5** were employed for product quantitation of electrolysis solutions.

(40) HRMS data were provided by the Midwest Center for Mass Spectrometry, University of Nebraska.

Acknowledgment. Grateful acknowledgment is made to the U.S. Department of Energy for supporting this research through Grant No. DE-FG22-80PC30227. Financial support to M.D.K. was made possible by a North Dakota MMRRI Fellowship. The authors thank Sylvia Farnum and David Miller of the UND Energy Research Center for generously providing NMR and GC-MS data. Appreciation is extended to Loren Linder for the synthesis of 4-cyanodiphenyl ether. Appreciation is also extended to Dilip Patil for preliminary synthesis of 2-cyanodiphenyl ether.

Registry No. 3, 1591-30-6; **4**, 96807-04-4; **5**, 96807-05-5; 2-phenoxybenzamide, 72084-13-0; 4-bromobenzonitrile, 623-00-7; potassium phenoxide, 100-67-4; 4-cyanodiphenyl ether, 3096-81-9; 2-cyanodiphenyl ether, 6476-32-0; 2-phenoxybenzoic acid, 2243-42-7.

The Chemistry of Free and Complexed Phosphirenes: Reactivity toward Electrophiles, Nucleophiles, and Conjugated Dienes

Angela Marinetti and François Mathey*

Contribution from the Laboratoire CNRS-SNPE, BP 28, 94320 Thiais, France.
Received January 25, 1985

Abstract: The direct conversion of phosphole into phosphirene complexes has been achieved by reaction of the former with dimethyl acetylenedicarboxylate and alkynes. The cleavage of the phosphirene ring in some P-$W(CO)_5$ complexes has been observed with basic water, morpholine, and methanol under UV. In all cases, vinylphosphorus compounds are obtained. A [4 + 2] Diels-Alder cycloaddition of 2,3-dimethylbutadiene with the double bond of 2-ethoxycarbonyl-1,3-diphenylphosphirene P-$W(CO)_5$ complex has given the expected bicyclic phosphirane. 1,2,3-Triphenylphosphirene obtained from the corresponding P-$W(CO)_5$ complex by decomplexation with iodine and *N*-methylimidazole reacts sluggishly with Me_3O^+, BF_4^- to give the 1-methylphosphirenium salt, which is instantly opened by neutral water at room temperature to give the corresponding vinylphosphine oxide. The same phosphirene reacts readily with *n*-butyllithium at −70 °C in THF to give the open-chain butylphenylphosphino-substituted vinyl carbanion as a mixture of cis and trans species. The reactions of this carbanion with water, methyl iodide, and *p*-chlorobenzaldehyde have been studied and always give a mixture of *Z* and *E* vinyl compounds, the trans attack being favored in each case. Triphenylphosphirene is also cleaved by sodium-naphthalene at −70 °C in THF. According to protonation and methylation experiments, the P,C dianion thus obtained does not isomerize.

The chemistry of heterocyclopropenes $XC_2R'_2$ is a field of considerable current interest. Whereas 1*H*-azirines (X = NR), oxirenes (X = O), and thiirenes (X = S) are still elusive species, stable borirenes (X = BR),[1-3] silirenes (X = SiR_2),[4-6] germirenes (X = GeR_2),[7] and thiirenium salts (X = S^+R)[8,9] have been discovered recently. There are at least three reasons why such rings deserve a special interest. Firstly, drastic changes of the reactivity of both the heteroatoms and the X-C bonds are expected due to the very high strain of these heterocycles. Secondly, various two- and four-electron stabilizing and destabilizing interactions between the carbon-carbon double bond and the heteroatoms can be envisaged and experimentally probed in such systems. Thirdly, these species are expected to be very versatile synthons through ring openings and ring expansions.

With such a background, phosphirenes (X = PR) were an obvious target for phosphorus chemists. The first attempted synthesis of this ring was reported by Stille.[10] The suspected 1,2,3-triphenylphosphirene oxide was later shown to be an open-chain product.[11] Then, Russian[12] and Indian chemists[13] claimed to have prepared pentacoordinate phosphirenes, but the data provided were so limited that the phosphirene structure cannot be considered established. In 1982, we reported the first unambiguous synthesis of the phosphirene ring, the existence of which was proven by X-ray crystal structure analysis.[14] The ring was

(1) van der Kerk, S. M.; Budzelaar, P. H. M.; van der Kerk-van Hoof, A.; van der Kerk, G. J. M.; von Ragué Schleyer, P. *Angew. Chem., Int. Ed. Engl.* **1983**, *22*, 48.
(2) Pues, C.; Berndt, A. *Angew. Chem., Int. Ed. Engl.* **1984**, *23*, 313.
(3) Pachaly, B.; West, R. *Angew. Chem., Int. Ed. Engl.* **1984**, *23*, 454.
(4) Conlin, R. T.; Gaspar, P. P. *J. Am. Chem. Soc.* **1976**, *98*, 3715.
(5) Hirotsu, K.; Higuchi, T.; Ishikawa, M.; Sugisawa, H.; Kumada, M. *J. Chem. Soc., Chem. Commun.* **1982**, 726.
(6) Seyferth, D.; Annarelli, D. C.; Vick, S. C. *J. Organomet. Chem.* **1984**, *272*, 123 and references cited herein.
(7) Krebs, A.; Berndt, J. *Tetrahedron Lett.* **1983**, *24*, 4083.
(8) Capozzi, G.; Lucchini, V.; Modena, G.; Scrimin, P. *Tetrahedron Lett.* **1977**, 911.
(9) Destro, R.; Pilati, T.; Simonetta, M. *Nouv. J. Chim.* **1979**, *3*, 533.
(10) Koos, E. W.; van der Kooi, J. P.; Green, E. E.; Stille, J. K. *J. Chem. Soc., Chem. Commun.* **1972**, 1085.
(11) Quast, H.; Heuschmann, M. *J. Chem. Soc., Chem. Commun.* **1979**, 390.
(12) Torgomy, A. M.; Ovakimyan, M. Zh.; Indzhikyan, M. G. *Arm. Khim. Zh.* **1979**, *32*, 288.
(13) Kansal, N. M.; Verma, S.; Mishra, R. S.; Bokadia, M. M. *Indian J. Chem.* **1980**, *19B*, 610. Verma, S.; Kansal, N. M.; Mishra, R. S.; Bokadia, M. M. *Heterocycles* **1981**, *16*, 1537.
(14) Marinetti, A.; Mathey, F.; Fischer, J.; Mitschler, A. *J. Am. Chem. Soc.* **1982**, *104*, 4484.

0002-7863/85/1507-4700$01.50/0